RSC Sustainability

ROYAL SOCIETY OF CHEMISTRY

PAPER

View Article Online
View Journal | View Issue

Cite this: *RSC Sustainability*, 2023, **1**, 1471

Convenient hydrogenation of furfural to furfuryl alcohol in metal-catalyzed and organo-catalyzed environments†

Asanda C. Matsheku, [a] Munaka Christopher Maumela[ab] and Banothile C. E. Makhubela *[a]

Palladium iminophosphorane (**C1–C3**) and pyridylimine (**C4–C5**) pincer complexes were evaluated for their activity in the conversion of furfural to furfuryl alcohol in the presence of triethylamine (Et_3N) and formic acid (FA). A catalyst loading of 0.1 mol% Pd afforded conversions of >99% achieving TONs of up to 9996. Surprisingly, upon evaluating a control blank (no metal catalyst) the conversions remained at >99% under metal catalyst-free conditions. Various tertiary and secondary amines were also screened in place of Et_3N and all proved efficient in furfural hydrogenation to furfural alcohol giving comparable conversions (>99%). Apart from furfural, metal catalyst-free hydrogenation was expanded to various other aldehydes all of which were converted to their corresponding alcohols in excellent yields of up to 100%. This work has led to a new discovery that would result in cost-effective metal catalyst-free processes for aldehyde hydrogenation.

Received 14th February 2023
Accepted 16th July 2023

DOI: 10.1039/d3su00056g

rsc.li/rscsus

Sustainability spotlight

Global energy deficiencies and environmental pollution have encouraged the need to advance to new technologies that are cost-effective towards the preparation of biofuels. Biomass is a valuable source of renewable carbon, and it can be converted to fuels and useful chemicals. Lignocellulosic biomass is the most convenient alternative source because it is renewable, non-edible, and can be transformed into upgradable platform molecules such as furfural. We focus on the selective hydrogenation of furfural to furfuryl alcohol for its versatility in the production of biofuels. Considering that we are already running short of liquid fuels required to run the economy, we have successfully transformed furfural into furfuryl alcohol with a shift from metal-catalyzed hydrogenation to organo-facilitated hydrogenation (without the use of a metal catalyst) in 6 hours in alignment with the UN sustainable development goals: affordable and clean energy (SDG 7) and climate action (SDG 13).

Introduction

Biomass is a valuable source of renewable carbon and it can be converted to fuels, useful chemicals and materials; however, the transformation methods that could unlock its full potential are not yet fully developed. This has encouraged researchers in academia and industry to explore ways to exploit biomass feedstock as a renewable alternative to produce value-added fuels and chemicals.[1]

Furfural (FFR) is one of the large-volume furan-based organic chemicals produced from non-edible lignocellulosic biomass – where the pentosans found in hemicellulose are transformed into FFR.[2,3] The global production of FFR is estimated to be around 370 000 tonnes per annum and its market price is USD $2200 per ton.[4,5] The largest FFR producer in the world is Central Romona located in the Dominican Republic while the second largest plant is owned by Illovo Sugar, in Sezela, Kwa-Zulu Natal, South Africa, and together they produce in excess of 50 000 Mt FFR per annum using bagasse as feedstock.[6]

Further chemical conversion of FFR can yield a variety of chemicals and fuels,[7] such as FFR alcohol, 2-methylfuran, levulinic acid, furoic acid and 2-methyltetrahydrofuran and tetrahydrofuran.[8] This is achieved mainly by selective catalytic hydrogenation, oxidation, hydrogenolysis and decarbonylation of FFR.[9–13]

Since FFR is an α,β-unsaturated carbonyl compound, where the C=C is located inside the furan ring, it is a suitable molecule for selective reduction of the carbonyl group (C=O), without saturating the C=C olefinic groups, affording furfural alcohol (Fig. 1).[14] Furfuryl alcohol (FFA) forms the primary chemical derived from the catalytic hydrogenation of FFR and

[a]*Research Centre for Synthesis and Catalysis, Department of Chemical Sciences, University of Johannesburg, Auckland Park, Kingsway Campus, 2006, South Africa. E-mail: ac.matsheku@gmail.com; bmakhubela@uj.ac.za; Tel: +27-11-559-3782*

[b]*Research and Technology, Sasol, 1 Klasie Havenga Rd, Sasolburg 1947, South Africa. E-mail: chris.maumela@sasol.com*

† Electronic supplementary information (ESI) available. CCDC 2092021. For ESI and crystallographic data in CIF or other electronic format see DOI: https://doi.org/10.1039/d3su00056g

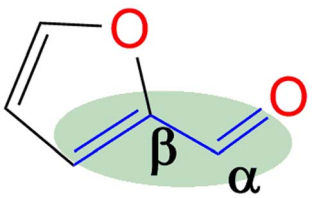

Fig. 1 Structure of FFR, showing its α,β-unsaturation.

its production has been estimated to take up to ~65% of all FFR produced.[15] It has important applications in the polymer industry which includes the production of rubbers, synthetic fibres, resins and agrochemicals. Moreover, it has been utilized in manufacturing fine chemicals, vitamin C, lubricants and lysine. FFA is also a chemical building block for drug synthesis and is used in the production of foundry sand binders.[2,16]

Selective reduction of carbonyl groups (such as the aldehyde in furfural) can be carried out catalytically or with stoichiometric amounts of reducing agents through transfer hydrogenation (TH). Such reducing agents, for example hydrides such as $NaBH_4$, $LiAlH_4$, and SiH_4 are air and moisture sensitive and challenging to handle.[17,18] In the past, there were studies on base-catalyzed reduction of carbonyl groups such as aldehydes because this would mean more sustainable metal catalyst-free reactions. However, these base-catalyzed reactions required harsh conditions (*e.g.* , 200 °C and >100 bar H_2) and reagents such as potassium *tert*-butoxide which limited wide-spread application.[19–21] As such, efforts focused on using inexpensive non-noble metal catalysts instead.

Several non-noble metal heterogeneous catalysts, including Cu/AC,[22] Ni/C,[23] RuNi/Fe_2O_4,[24] and NiW/C[25] MgO/Fe_2O_4 (ref. 26) have been used to convert FFR into a mixture of FFA, 2-methyl furan and tetrahydrofurfural alcohol. This multiple product formation requires unwanted additional separation steps to obtain pure FFA.[27–30]

The industrially used copper chromate catalyst is selective at converting FFR into FFA in the gaseous phase; however the use of environmentally toxic chromium is of concern,[31,32] necessitating the development of efficient, non-toxic catalysts that function under mild conditions.

Common hydrogen donors such as isopropanol, ethanol, methanol and formic acid are widely used with metal catalysts in TH, specifically, ruthenium,[33] iridium,[34] platinum,[35] palladium,[36] iron,[37] manganese[38] and nickel[39] homogeneous catalysts. The versatile tridentate architecture of pincer ligands has been identified as effective in altering and regulating metal complex characteristics across the periodic table.[40–46]

Initially, in this study, iminophosphorane and pyridylimine palladium(II) pincer complexes were used as homogeneous catalyst precursors for the selective hydrogenation of FFR to FFA. In the course of the study we discovered that this reaction proceeds without the metal catalyst – in the presence of *in situ* generated formate, produced from formic acid and the amine. Therefore, we have demonstrated a convenient method to selectively hydrogenate aldehydes to alcohols that moves from palladium homogeneous catalysts to organocatalysed formate hydrogenations.

Experimental details

Materials and methods

All experiments were conducted in air unless otherwise stated. The solvents used were of reagent grade and not distilled prior to use unless otherwise stated. All chemicals were purchased from Sigma Aldrich and used as received; however, the solvents were kept anhydrous in molecular sieves. These include 2,6-pyridinemethanol, triphenylphosphine, 4-(diphenylphosphine) carboxylic acid, sodium azide, 4-aminobenzoic acid, 2,6-(diformyl)pyridine, triethylamine and other chemicals used herein. $PdCl_2$ was purchased from Heraeus South Africa and used as received. $[PdCl_2(MeCN)_2]$ was synthesized according to literature procedures.[47] ^{1}H NMR spectra were recorded on a Bruker-400 MHz spectrometer (^{1}H at 500 MHz and $^{13}C\{^1H\}$ at 100 MHz). The chemical shift values were reported relative to the internal standard tetramethylsilane (δ 0.00). These were referenced to the residual proton and carbon signals at δ 7.24 and 77.0 ppm respectively of $CDCl_3$. Similarly, for DMSO-d_6, the reference for the residual proton and carbon signals were at δ 2.49 and 39.0 ppm respectively. Analytical thin layer chromatography (TLC) was performed using silica gel coated aluminium plates (0.2 mm). The developed plates were then analysed through visualization under UV light or iodine staining. Silica gel column chromatography was performed using silica gel 60 (70–230 mesh). FT-IR spectra (between 4000 and 600 cm^{-1}) were recorded as ATR using a PerkinElmer BX (II) spectrometer. Elemental analyses were conducted using a Thermos Scientific Flash 2000 CNHSO analyser. ESI-MS was carried out at Stellenbosch University Central Analytical Services using a Waters Synapt G2 and melting points were determined using the Gallenkamp Digital Melting-Point Apparatus 5A 6797. XRD spectra were obtained from a Bruker APEX-II CCD diffractometer.

The single crystal X-ray analysis

Single crystal X-ray diffraction data were obtained using a Bruker APEXII diffractometer with Mo Kα (λ = 0.71073 Å) radiation and at a detector to crystal distance of 4.00 cm. The initial cell matrix was obtained from three series of scans at different starting angles. Each series consisted of 12 frames collected at intervals of 0.5° in a 6° range, with an exposure time of about 10 s per frame. The reflections were successfully indexed using an automated indexing routine built in the APEXII program suite. The data were collected using the full sphere data collection routine to survey the reciprocal space to the extent of a full sphere, with a resolution of 0.75 Å. Data were obtained by collecting 2982 frames at intervals of 0.5° scans in ω and ϕ with an exposure time of 10 s per frame.[48] The data integration and reduction were processed with SAINT software. A multi-scan absorption correction was applied to the collected reflections with SADABS using XPREP. Structures were solved by direct methods using the program SHELXS-97 and were refined on F2 by the full-matrix least-squares technique using the SHELXL-97 program package. All non-hydrogen atoms were refined with anisotropic displacement coefficients. All hydrogen

atoms were included in the structure factor calculations at idealized positions and were allowed to ride on the neighbouring atoms with relative isotropic displacement coefficients.[49]

2,6-Bis(chloromethyl)pyridine (1).[50]

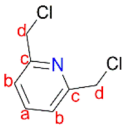

2,6-Pyridinedimethanol (2.40 g, 17.3 mmol) was added slowly to 20 mL of thionyl chloride ($SOCl_2$) at 0 °C. The reaction mixture was stirred at room temperature for an hour and was then refluxed at 80 °C for 2 hours. The crude mixture was concentrated under vacuum and thereafter 20 mL of H_2O was added slowly. The solution was filtered, and a saturated aqueous solution of sodium bicarbonate was added dropwise into the filtrate until there was no sign of bubbling to obtain a precipitate. The precipitate was isolated by filtration to afford 2,6-bis(chloromethyl)pyridine (**1**) as a white solid. Yield: 2.2 g, 92%. Melting point: 74–76 °C. ^{1}H NMR (400 MHz, $CDCl_3$, 25 °C): δ 4.81 (s, 4H, H_d), 7.58 (d, $J = 7.8$ Hz, 2H, H_b), 7.93 (t, $J = 7.8$ Hz, 1H, H_a).

2,6-Bis(azidomethyl)pyridine (2).[51]

2,6-Bis(chloromethyl)pyridine (**1**) (1.00 g, 6.76 mmol) was dissolved in DMSO (20 mL) and NaN_3 (0.878 g, 13.5 mmol) was added. This reaction mixture was then stirred at room temperature for 24 hours. The crude mixture was quenched with 20 mL of water followed by washing with diethyl ether (3 × 50 mL). The diethyl ether layer (150 mL) was then collected and washed with brine (2 × 100 mL). The organic layer was collected and dried with anhydrous magnesium sulfate for 30 minutes. After drying, $MgSO_4$ was removed by filtration and the solvent was removed from the filtrate, using a rotary evaporator, to obtain (**2**) as a yellow oil, which was dried under vacuum for 2 hours. Yield: 0.912 g, 71%.[51] ^{1}H NMR (400 MHz, $CDCl_3$, 25 °C): δ 4.65 (s, 4H, H_d), 7.41 (d, $J = 7.8$ Hz, 2H, H_b), 7.73 (t, $J = 7.6$ Hz, 1H, H_a).

***N*,*N*′-(Pyridine-2,6-diylbis(methylene))bis(1,1,1-triphenyl-l5-phosphanimine) (L1).**

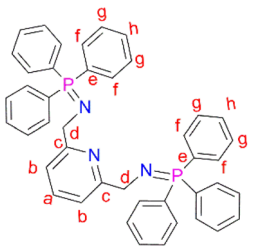

N,*N*′-(Pyridine-2,6-diylbis(methylene))bis(1,1,1-triphenyl-l5-phosphanimine) (**L1**) was prepared by adding triphenylphosphine (0.831 g, 3.17 mmol) to a solution of (**2**) (0.300 g, 1.58 mmol) in 30 mL diethylether into a Schlenk tube. The resultant solution was then stirred at room temperature, under N_2 gas, for 16 hours, during which time a white precipitate formed. After 16 hours, a white solid was collected by vacuum filtration and dried under vacuum for 5 hours to afford ligand **L1**. Yield: 0.705 g, 68%.[51] Melting point: 120–123 °C. ^{1}H NMR (400 MHz, $CDCl_3$, 25 °C): δ 4.38 (d, $J = 12$ Hz, 4H$_d$), 7.35 (td, $J = 4$–8 Hz, 12 H$_g$), 7.43 (td, $J = 4$ Hz, 6H$_h$), 7.59 (br t, $J = 4$–12 Hz, 1H$_a$), 7.63–7.67 (br t, $J = 8$ Hz, 12H$_f$), 7.70 (br d, $J = 4$ Hz, 2H$_b$). ^{13}C{^{1}H} NMR (101 MHz, $CDCl_3$) δ 51.12 (C_d), 118.18 (C_b), 128.28 (C_g), 131.13 (C_h), 132.02 (C_e), 132.49 (C_f), 136.60 (C_a), 153.59 (C_c). ^{31}P{^{1}H} NMR (162 MHz, $CDCl_3$) δ 12.39 (s). IR (cm^{-1}): 1587 ν(C=N), 1330 ν(P=N), 1103 ν(C–N). Elemental analysis: calculated for $C_{43}H_{37}N_3P_2$ (%): C 78.52, H 5.44, N 5.67. Found: C 77.10, H 5.47, N 6.34. HR-ESI-MS(+): $m/z = 657.1031$ [M]$^+$.

4,4′-(Pyridine-2,6-diylbis(methylene))bis(azaneylylidene))bis(diphenyl-l5-phosphaneylylidene))dibenzoate (L2).

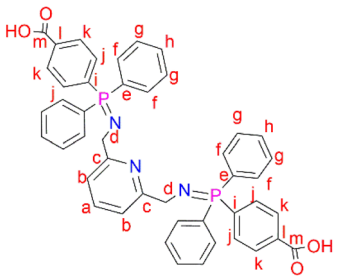

2,6-Bis(azidomethyl)pyridine (**2**) (0.200 g, 1.06 mmol) was added to a solution of 4-(diphenylphosphino) benzoic acid (0.647 g, 2.11 mmol) dissolved in dichloromethane (20 mL). The resulting solution was then refluxed at 40 °C for 24 hours, during which time a yellow precipitate formed. The yellow solid (**L2**) was obtained, following vacuum filtration of the suspended precipitate, and dried under vacuum for 2 hours. Yield: 0.708 g, 90%. Melting point: 209–212 °C. ^{1}H NMR (400 MHz, D_2O and NaOD, 25 °C): δ 7.55 (br d, $J = 3.0$ Hz, 4H, H_k), 7.42 (br s, 1H, H_a), 7.09 (br s, 4H, H_j), 7.00 (br m, 12H, $H_{g,h}$), 6.92 (br d, $J = 6.0$ Hz, 2H, H_b), 6.85 (br s, 8H, H_f), 3.49 (br s, 4H, H_d). ^{13}C{^{1}H} NMR (400 MHz, D_2O and NaOD, 25 °C): δ 45.7 (C_d), 119.7 (C_b), 128.5–129.1 (C_k, C_g, C_j), 129.8 (C_h), 131.2–131.5 (C_f), 132.3 (C_e), 132.7 (C_a), 138.8 (C_l), 140.5 (C_i), 160.3 (C_c), 173.3 (C_m). ^{31}P{^{1}H} NMR (162 MHz, D_2O and NaOD, 25 °C): δ 34.2. FT-IR (cm^{-1}): 3454 ν(O–H), 1735 ν(C=O), 1595 ν(C=N), 1363 ν(P=N), 1110 ν(C–N). Elemental analysis: calculated for C_{45} H_{37} N_3 O_4 P_2 (%): C 72.48, H 5.00, N 5.63. Found: C 71.51H 5.23, N 5.35. HR-ESI-MS(+): ($C_{45}H_{37}N_3O_4P_2$) $m/z = 745.2189$ [M]$^+$.

***para*-Aminobenzoic acid methyl ester (3).**[52,53]

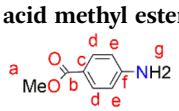

A solution of *p*-aminobenzoic acid (6.0 g, 43.8 mmol) in 40 mL MeOH was cooled to 0 °C, and thionyl chloride (7.95 mL, 109 mmol) was added dropwise to the solution. The reaction solution was heated at reflux for 24 hours after which it was cooled to room temperature. The solvent was reduced under pressure to give a residue, to which $NaHCO_3$ solution (100 mL) was added. The product was extracted using ethyl acetate (3 × 20 mL), and then the ethyl acetate layers were combined and dried over anhydrous magnesium sulfate. After purification using a gel silica-packed column eluting with *n*-hexane : EtOAc, in a 1 : 1 ratio, *para*-amino benzoic acid methyl ester (**3**) was afforded as a white solid. Yield: 5.94 g, 89%. Melting point: 106–108 °C. ^{1}H NMR (400 MHz,

$CDCl_3$, 25 °C): δ 7.82 (d, $J = 8.8$ Hz, 2H, H_d), 6.61 (d, $J = 8.8$ Hz, 2H, H_e), 4.06 (br s, 2H, H_g), 3.83 (s, 3H, H_a). $^{13}C\{^1H\}$ NMR (101 MHz, $CDCl_3$, 25 °C): δ 167.1 (C), 150.8 (C), 131.6 (C), 119.7 (C), 113.7 (C), 51.6 (C). HR-ESI-MS(+): m/z = 150.0547 $[M]^+$.

4-(Diphenylphosphino)aminomethylbenzoate (4).

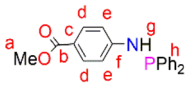

4-Dimethylaminopyridine (DMAP) (0.242 g, 1.98 mmol) and Et_3N (2.76 mL, 19.8 mmol) were added to a solution of the starting material (**3**) (1.5 g, 9.92 mmol) in dry THF (10 mL) under N_2. The solution was stirred for 1 hour and then cooled to 0 °C, after which chlorodiphenylphosphine (1.78 mL, 9.98 mmol) was added. The resultant solution was stirred further for 18 hours at room temperature. After 18 hours, the solvent was removed *in vacuo* and the crude product was dissolved in dry ethanol (15 mL). This resulted in the formation of a precipitate that was isolated by filtration and dried under vacuum, for 9 hours, to afford the phosphine (**4**) as a white solid. Yield: (3.0 g, 90%). Melting point: 87–89 °C. ^1H NMR (400 MHz, $CDCl_3$, 25 °C): δ 7.87 (d, $J = 8.8$ Hz, 2H, H_d), 7.46–7.39 (m, 4H, H_h), 7.37 (d, $J = 2.8$ Hz, 6H, H_h), 7.00 (d, $J = 10.8$ Hz, 2H, H_e), 4.70 (d, $J = 7.5$ Hz, 1H, H_g), 3.84 (s, 3H, H_a). (s). $^{13}C\{^1H\}$ NMR (101 MHz, $CDCl_3$, 25 °C): δ 166.99 (C), 151.24 (C), 151.07 (C), 139.13 (C), 139.02 (C), 131.34 (C), 131.2 (2C), 131.08 (2C), 129.37 (2C), 128.66 (2C), 128, 59 (2C), 120.79 (C), 115.08 (C), 114.95 (C), 51.58 (C). $^{31}P\{^1H\}$ NMR (162 MHz, $CDCl_3$, 25 °C): δ 28.39. FT-IR (cm^{-1}): ν(N–H), 3264, ν(C=O) 1681, ν(P–Ph) 1443, ν(P–N) 959. HR-ESI-MS(+): m/z = 336.1160 $[M + H]^+$.

Dimethyl-4,4′-((((pyridine-2,6 diylbis(methylene))bis(azaneylylidene))bis(diphenyl-l5-phosphaneylylidene)) bis(azanediyl))dibenzoate (L3).

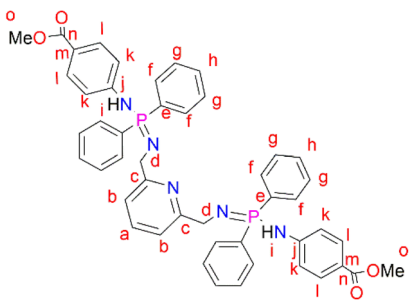

2,6-Bis(chloromethyl)pyridine (**2**) (0.112 g, 0.596 mmol) was dissolved in THF (20 mL) followed by the addition of (**3**) (0.400 g, 1.19 mmol) under nitrogen in a Schlenk tube. This reaction mixture was allowed to stir at room temperature for 48 hours. The resulting reaction mixture was filtered through alumina and the solvent was removed from the filtrate to isolate a pale-yellow solid, **L3** (very sensitive to air and moisture) that was dried under vacuum for 8 hours. Yield: 0.122 g, 26%. ^1H NMR (400 MHz, $CDCl_3$, 25 °C): δ 7.91 (br t, $J = 8$ Hz, 8H, H_g), 7.81 (br d, $J = 8$ Hz, 1H, H_a), 7.66 (d, $J = 4$ Hz, 4H, H_l), 7.44 (br d, $J = 4$ Hz, 4H, H_h), 7.37 (br s, 8H, H_f), 6.93 (d, $J = 4$ Hz, 2H, H_b), 6.83 (d, $J = 4$ Hz, 4H, H_k), 4.39 (br s, 2H, H_i), 3.83 (s, 4H, H_d), 3.77 (s, 6H, H_o). $^{31}P\{^1H\}$ NMR (162 MHz, $CDCl_3$, 25 °C): δ 7.80 (s). HR-ESI-MS(+): m/z = 804.2887 $[M + H]^+$.

4,4′-(((1*E*,1′*E*)-Pyridine-2,6-diylbis(methaneylylidene)) bis(azaneylylidene))diphenol (L4).

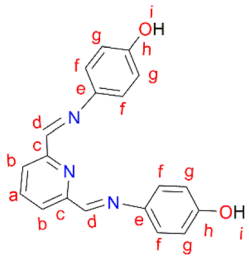

2,6-Diformylpyridine (0.100 g, 0.740 mmol) was dissolved in methanol and added to a stirring solution of 4-aminophenol (0.177 g, 0.163 mmol) in methanol, followed by the addition of 5–8 drops (0.4 mL) of acetic acid. The reaction solution was then refluxed at 45 °C for 16 hours, during which time a yellow precipitate formed. The yellow precipitate, **L4**, was collected by suction filtration and dried under vacuum for 6 hours. Yield: 0.226 g, 99%. Melting point: 137–140 °C. ^1H NMR (500 MHz, DMSO-d_6, 25 °C) δ: 6.82 (d, $J = 10$ Hz, 4H, H_g), 7.32 (d, $J = 10$ Hz, 4H, H_f), 8.03 (t, $J = 5$–10 Hz, 1H, H_a), 8.17 (d, $J = 5$ Hz, 2H, H_b), 8.66 (s, 2H, H_d), 9.66 (br s, 2H, H_i). $^{13}C\{^1H\}$ NMR (101 MHz, DMSO-d_6, 25 °C) δ: 118.4 (C_g), 124.3 (C_b), 129.5 (C_f), 137.3 (C_a), 143.6 (C_e), 148.6 (C_c), 155.9 (C_d), 166.9 (C_h). FT-IR (cm^{-1}): 3520 ν(OH), 1566 ν(C=N), 1620 ν(C=N). Elemental analysis: calculated for C_{19} H_{15} N_3 O_2 (%): C 71.91, H 4.76, N 13.24. Found: C 69.95, H 6.13, N 12.94. HR-ESI-MS(+): m/z = 320.1008 $[M + H]^+$.

4,4′-(((1*E*,1′*E*)-Pyridine-2,6-diylbis(methaneylylidene)) bis(azaneylylidene))dibenzoate (L5).

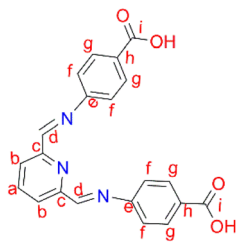

2,6-Diformylpyridine (0.100 g, 0.740 mmol) was added to stirring solution of 4-aminobenzoic acid (0.224 g, 0.163 mmol) in methanol and the same protocol as outlined for the synthesis of ligand **L4** was followed. A white solid of ligand **L5** was isolated after drying under vacuum for 8 hours. Yield: 0.249 g, 96%. Melting point: >300 °C. ^1H NMR (400 MHz, D_2O and NaOD, 25 °C) δ: 5.99 (br s, 2H, H_d), 6.59 (d, $J = 10$ Hz, 4H, H_f), 7.29 (d, $J = 10$ Hz, 2H, H_b), 7.51 (d, $J = 5$ Hz, 4H, H_g), 7.67 (t, $J = 5$–10 Hz, 1H, H_a). $^{13}C\{^1H\}$ NMR (400 MHz, D_2O and NaOD, 25 °C): δ 114.9 (C_f), 119.6 (C_b), 126.0 (C_h), 130.8 (C_g), 138.4 (C_a), 149.7 (C_c), 161.2 (C_d), 175.5 (C_i). FT-IR (cm^{-1}): 3096 ν(OH), 1680 ν(C=O), 1598 ν(C=N), 1572 ν(C=N). Elemental analysis: calculated for C_{21} H_{15} N_3 O_4 (%): C 67.56, H 4.05, N 11.25. Found: C 67.42, H 4.13, N 11.32 HR-ESI-MS(+): m/z = 374.1138 $[M]^+$.

[PdCl(L1)]BPh$_4$, (C1).

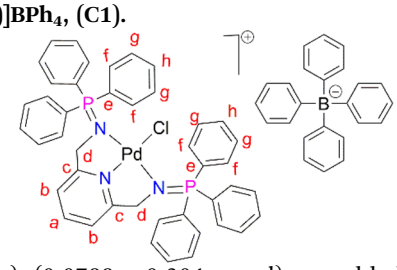

$PdCl_2(CNMe)_2$ (0.0788 g, 0.304 mmol) was added to a stirring solution of **L1** (0.200 g, 0.304 mmol) in 20 mL of methanol. This yellow solution formed was then stirred, under nitrogen, at room temperature for 24 hours. After 24 hours, a green solution formed and the solvent was reduced to ~5 mL before adding sodium tetraphenylborate ($NaBPh_4$) (0.104 mg, 0.304 mmol) and stirring for a further 30 minutes, at room temperature. After 30 minutes, a pale green precipitate (**C1**) had formed, that was collected using suction filtration before drying under vacuum for 8 hours. Yield: (0.309 g, 91%). Melting point: decomposes without melting, onset occurs at 215 °C. ^{1}H NMR (400 MHz, CD_3CN, 25 °C) δ: 4.35 (d, J = 5 Hz, 4H, H_d), 6.82 (t, J = 5–10 Hz, 4H, H_l), 6.97 (t, J = 5–10 Hz, 8H, H_k), 7.06 (d, J = 5 Hz, 2H, H_b), 7.25 (br m, 8H, H_j), 7.54–7.58 (t d, J = 5 Hz, 12H_f), 7.66 (t d, J = 5 Hz, 6H, H_h), 7.72 (t, J = 8 Hz, 1H, H_a), 7.82–7.86 (br m, 12H, H_g). ^{13}C{^{1}H} NMR (101 MHz, CD_3CN, 25 °C) δ: 62.5 (C_d), 119.6 (C_b), 123.2 (C_l), 126.9 (C_k), 127.3 (C_g), 128.1 (C_e), 130.0 (C_h), 134.3 (C_j), 135.2 (C_f), 137.2 (C_a), 139.9 (C_i), 165.2 (C_c). ^{31}P{^{1}H} NMR (162 MHz, CD_3CN) δ: 35.49. FT-IR (cm^{-1}): 1575 ν(C=N), 1261 ν(P=N), 1110 ν(C–N). Elemental analysis: calculated for $C_{67}H_{57}BClN_3P_2Pd$ (%): C 71.93 H, 5.14 N, 3.76. Found: C, 71.51 H, 5.03 N, 3.84. HR-ESI-MS(+): m/z = 798.1198 [M]$^+$.

[PdCl(L2)]Cl, (C2).

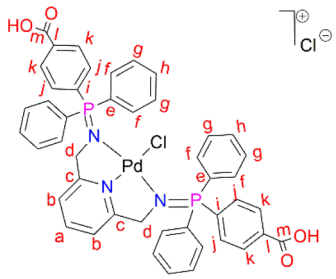

L2 (0.500 g, 0.670 mmol) was added to a Schlenk flask containing $PdCl_2(CNMe)_2$ (0.173 g, 0.670) in acetonitrile, followed by 5–10 drops (0.5 mL) of acetic acid. The resulting solution was then stirred, under nitrogen, at room temperature for 72 hours. Thereafter, the solvent was removed to isolate an orange-red solid that was desired under vacuum for 10 hours. Yield: 0.556 g, 90%). Melting point: 231–234 °C, melts with decomposition. ^{1}H NMR (500 MHz, DMSO-d_6, 25 °C) δ: 4.42 (br s, 4H, H_d), 7.33 (d, J = 10 Hz, 2H, H_b), 7.59 (m, 8H, H_g), 7.62 (br m, 4H, H_h), 7.80 (br m, 8H, H_f), 7.82 (br m, 12H, H_f), 7.88 (br t, J = 5–10 Hz, 1H, H_a), 8.07 (br d, J = 5 Hz, 4H, H_k). ^{13}C{^{1}H} NMR (101 MHz, DMSO-d_6) δ: 62.4 (C_d), 119.1 (C_b), 125.4 (C_l), 126.2 (C_k), 129.4 (C_g), 131.8 (C_h), 133.5 (C_j), 134.1 (C_f), 135.5 (C_i), 139.4 (C_a), 163.3 (C_c), 167.2 (C_l). ^{31}P{^{1}H} NMR (162 MHz, DMSO-d_6, 25 °C) δ: 34.64. FT-IR (cm^{-1}): 3433 ν(O–H), 1712 ν(C=O), 1581 ν(C=N), 1242 ν(P=N), 1103 ν(C–N). Elemental analysis: calculated for $C_{45}H_{37}Cl_2N_3O_4P_2Pd$ (%): C, 58.55 H, 4.04 N, 4.55. Found: C, 59.24 H, 4.16 N, 3.99. HR-ESI-MS(+): m/z = 888.0969 [M]$^+$.

[PdCl(L3)]Cl, (C3).

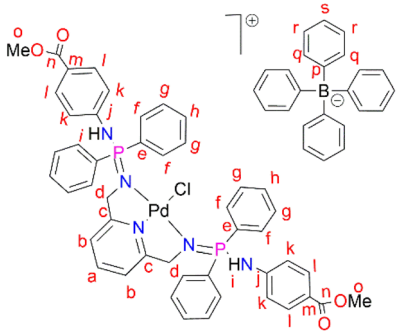

$PdCl_2(CNMe)_2$ (0.0722 g, 0.286 mmol) was added to a stirring solution of **L3** (0.230 g, 0.286 mmol) containing 20 mL of methanol. The resulting solution was stirred for 24 hours at room temperature, under nitrogen. After 24 hours, the solvent was removed, using a rotary evaporator, and the resulting solid was re-dissolved in methanol (5 mL) followed by the addition of $NaBPh_4$ (0.0979 g, 0.286 mmol). Thereafter, the solution was stirred at room temperature for 30 minutes, during which time a mustard solid (**C3**) formed. Complex **C3** was isolated using suction filtration and dried under vacuum for 6 hours. Yield: 0.108 g, 30%). Melting point: 159–163 °C. ^{1}H NMR (400 MHz, $CDCl_3$, 25 °C) δ: 7.78 (d, J = 4 Hz, 4H, H_l), 7.67 (br s, 12H, H_r, H_s), 7.43 (br s, 9H, H_a, H_q), 7.29 (br m, 8H, H_g), 7.03 (br s, 2H, H_b) 6.87 (br s, 8H, H_f), 6.77 (br s, 4H, H_h), 6.72 (d, J = 4 Hz, 4H, H_k), 6.15 (br d, J = 4 Hz, 2H, H_i), 4.07 (br d, J = 4 Hz, 4H, H_d), 3.84 (br s, 6H, H_o). ^{13}C{^{1}H} NMR (101 MHz, $CDCl_3$, 25 °C) δ: 52.0 (C_d), 60.5 (C_o), 118.6 (C_k), 119.5 (C_b), 121.8 (C_s), 124.7 (C_m), 125.5 (C_r), 127.2 (C_r), 128.3 (C_e), 128.7 (C_h), 129.5 (C_g), 131.0 (C_l), 132.8 (C_f), 134.0 (C_q), 136.2 (C_a), 139.3 (C_p), 144.0 (C_j), 164.4 (C_c), 166.6 (C_n). ^{31}P{^{1}H} NMR (162 MHz, $CDCl_3$, 25 °C) δ: 40.36 ppm. FT-IR (cm^{-1}): 3459 ν(N–H), 1718 ν(C=O), 1607 ν(C=N), 1232 ν(P=N), 1114 ν(C–N). Elemental analysis: calculated for C_{76} H_{70} BCl N_5 O_5 P_2 Pd (%);: C 67.42, H 5.02, N 5.54. Found: C 66.35, H 4.69, N 5.19 HR-ESI-MS(+): m/z = 944.1520 [M]$^+$

[PdCl(L4)]Cl, (C4).

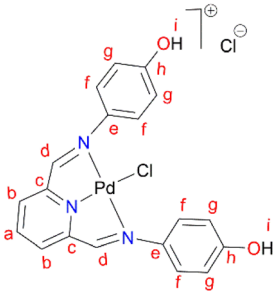

In a round bottom flask, $PdCl_2(CNMe)_2$ (0.0855 g, 0.329 mmol) was added to a stirring solution of **L4** (0.100 g, 0.329 mmol) containing 20 mL of methanol. The resulting reaction solution was refluxed at 65 °C for 24 hours, during which time a red precipitate formed. The precipitate (**C4**) was isolated using suction filtration and washed with MeOH forming a greenish solid that was dried under vacuum for 6 hours. Yield: 0.112 g,

68.7%). Melting point: decomposes without melting, onset occurs at 291 °C. ^{1}H NMR (500 MHz, DMSO-d_6) δ: 6.83 (d, J = 5 Hz, 4H, H_g), 7.34 (br m, 4H, H_f), 8.17 (br s, 1H, H_b), 8.50 (br s, 2H, H_d), 8.66 (s, 1H, H_a), 9.68 (br s, 1H, $H_{i'}$), 10.18 (br s, 1H, H_i). ^{13}C{^{1}H} NMR (101 MHz, DMSO-d_6) δ: 115.4 (C_g), 122.3 (C_f), 126.0 (C_b), 129.3 (C_a), 141.8 (C_e), 155.0 (C_c), 156.6 (C_h), 157.6 (C_d). FT-IR (cm^{-1}): 3325 ν(OH), 3526 ν(OH), 1550 ν(C=N), 1589 ν(C=N). HR-ESI-MS(+): m/z = 499.0456 [M]$^+$.

[PdCl(L5)]Cl, (C5).

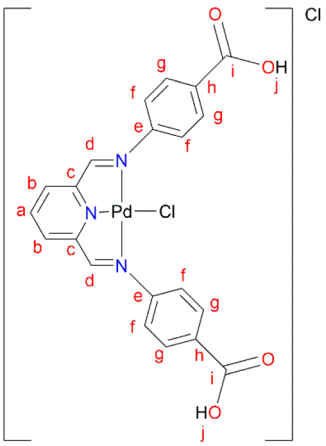

L5 (0.3300 g, 0.859 mmol) was added to a Schlenk flask containing $PdCl_2(CNMe)_2$ (0.223 g, 0.859 mmol) in MeOH, followed by 4–8 drops of acetic acid. The reaction mixture was allowed to stir at room temperature for 72 hours. A green precipitate was observed and isolated by vacuum filtration and then dried under vacuum for 8 hours, **C5** (0.260 g, 55%). Melting point: 297 °C, onset decomposition. ^{1}H NMR (500 MHz, DMSO-d_6) δ 5.86 (br s, 3H, Ar–H), 6.53 (br s, 3H, Ar–H), 7.13 (br s, 1H, Ar–H) 7.31 (br s, 1H, Ar–H), 7.60 (br s, 3H, $H_{a,b}$), 8.00 (br s, 2H, H_d), 12.22 (br s, 2H, H_j). ^{13}C{^{1}H} NMR (101 MHz, DMSO-d_6) δ 112.9 (C_f), 117.3 (C_b), 123.2 (C_a), 127.3 (C_h), 131.5 (C_g), 146.5 (C_c), 153.4 (C_e), 167.3 (C_i), 167.8 (C_d). FT-IR (cm^{-1}): 3282 ν(OH), 1681 ν(C=O), 1606 ν(C=N), 1575 ν(C=N).). HR-ESI-MS: m/z = 561.8280 [M + H]$^+$.

The general procedure for hydrogenation reactions

Substrate (furfural, 5 mmol), formic acid (5 mmol), catalyst (0.1–0.01 mol%), and base (Et_3N, 5 mmol) were added to an autoclave reactor. The homogeneous mixture was heated to the desired temperature after purging five times with nitrogen gas. The mixture was then left to stir for the required amount of time. At the end of the reaction, the reactor vessel was cooled and the gas generated was released. All hydrogenation reactions were carried out in triplicate. The end-of-reaction contents (crude mixture) containing the product were analyzed by ^{1}H NMR spectroscopy by sampling 0.1 mL, added to 0.4 mL of $CDCl_3$ and 5 μL of DMF was used as an internal standard to determine the amount of product (furfuryl alcohol) formed, and confirmed by GC-MS. The calculations were conducted following literature protocols.[16,25]

Results and discussion

Ligands, **L1–L3**, were prepared following a modified literature protocol reported by Cheisson and Auffrant.[51] The preparations are summarized in Scheme 1 which proceeded by first chlorinating 2,6-pyridinedimethanol to afford 2,6-bis(chloromethyl) pyridine (**1**), followed by a nucleophilic substitution reaction, with sodium azide as the nucleophile. This reaction led to isolation of 2,6-bis(azidomethyl)pyridine (**2**). The azide (**2**) was treated with various phosphines in a Staudinger reaction to afford ligands **L1–L3** in moderate to excellent yields (68–90%). The preparation of **L3** commenced by initially preparing 4-aminomethylbenzoate (**3**) by acid-catalyzed esterification of the carboxylic acid functional group in 4-aminobenzoic acid. Once (**3**) was obtained, 4-(diphenylphosphino) aminomethylbenzoate (**4**) was prepared by reacting (**3**) with chlorodiphenylphosphine at room temperature (Scheme 1). 4-(Diphenylphosphaneyl) aminomethylbenzoate (**4**) undergoes a facile Staudinger reaction to afford ligand **L3**. **L3** turned out to be air- and moisture-sensitive, therefore prone to oxidation which may be due to the *–NH* spacer. **L1** is stable but oxidizes when exposed to air/moisture for hours and **L2** is very stable. **L1** and **L3** were isolated as white powders respectively, which are soluble in chlorinated organic solvents, THF, DMSO, DMF and acetonitrile. **L2** was isolated as a pale-yellow solid that is very insoluble and requires deprotonation of the carboxylic groups by sodium hydroxide in water to encourage solubility. **L3** is very air and

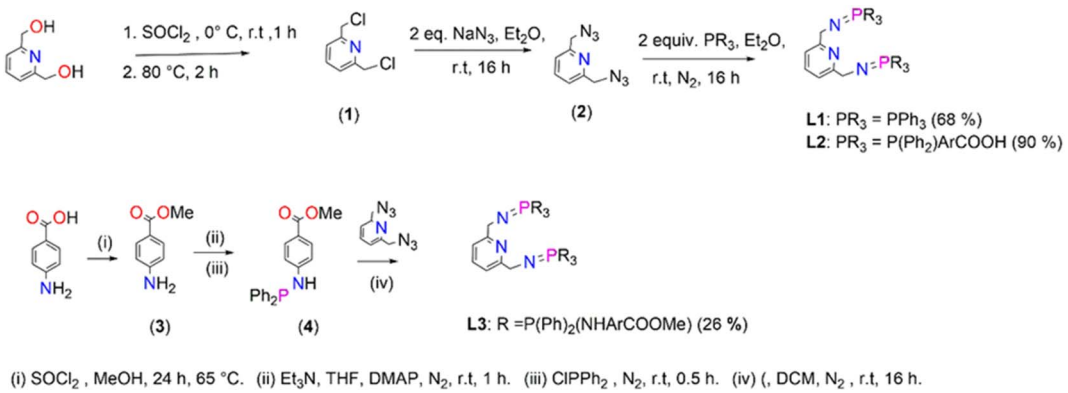

Scheme 1 The synthesis of iminophosphorane pincer ligands, L1–L3.

moisture sensitive, and upon exposure changes colour from a white powder to yellow oil as a result of oxidation.

(1), **(2)** and **L1** are known compounds.[51,54] **(1)** was confirmed by proton NMR, with four protons observed as a singlet at 4.81 ppm assigned to the chemically equivalent aliphatic protons –CH_2's. The proton NMR for **(2)** reveals a singlet at 4.65 ppm (a shift from 4.81 ppm **(1)**) which integrates for four protons assigned to the chemically equivalent –CH_2's and this agrees with that reported in the literature at 4.48 ppm (ESI-Fig. 1†). These protons (–CH_2) appear as a doublet in the proton NMR spectrum of **L1** seen at 4.38 ppm (ESI-Fig. 2†), in agreement with literature findings. Furthermore, the phosphorus NMR spectrum revealed a singlet at 12.4 ppm which is similar to literature reports at 9.9 ppm.[51] The proton NMR spectrum of **L2** revealed broadness in all expected characteristic peaks and this maybe due to the sodium counter ions as NMR could only be conducted upon deprotonation of the carboxylic –OH group using deuterated water and sodium hydroxide (ESI-Fig. 3†). The ^{13}C NMR spectrum revealed all the expected signals (ESI-Fig. 4†). The phosphorus NMR signals resonate at 34.2 ppm. The FT-IR spectroscopy of **L2** confirmed the expected characteristic vibrations; 3454 ν(O–H), 1735 ν(C=O), 1595 ν(C=N), 1363 ν(P=N), and 1110 ν(C–N) (ESI-Fig. 5†). The mass spectrum further confirms that **L2** was isolated successfully by revealing the parent ion $m/z = 745.2189$ $[M]^+$.

The proton NMR spectrum for **(3)** revealed a new singlet at 3.83 which corresponds to the successful formation of the methoxy group. The phosphorus NMR spectrum of **(4)** revealed a singlet that shows signals at 28.4 ppm (ESI-Fig. 6†). The formation of **L3** was monitored by phosphorus NMR due to the air and moisture sensitivity nature which encouraged the one pot synthesis of **L3** and its corresponding palladium complex **C3**. The phosphorus NMR spectrum of **L3** depicted a singlet at 7.80 ppm (ESI-Fig. 7†).

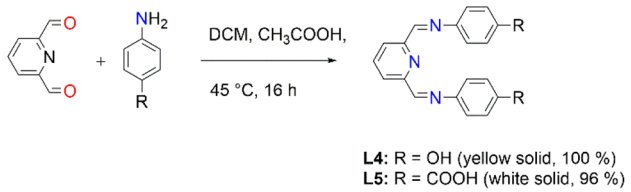

Fig. 2 The synthesis of Schiff-base ligands, **L4** and **L5**.

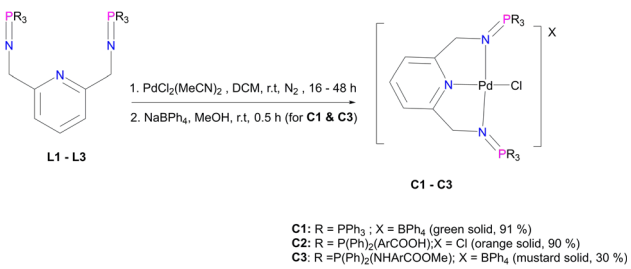

Fig. 3 The synthesis of iminophosphorane palladium pincer complexes, **C1–C3**.

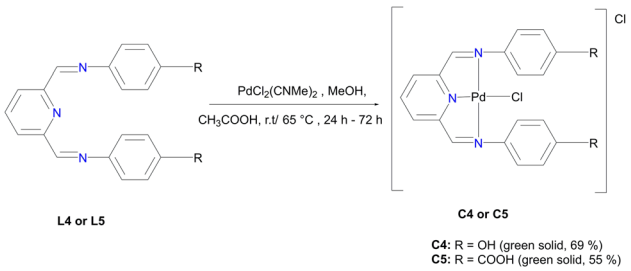

Fig. 4 The preparation of Pd-imine pincer complexes, **C1** and **C2**.

Moreover, the Schiff-base ligands **L4** and **L5** were also prepared following a modified literature protocol by Cvijetic and co-workers (Fig. 2).[55] **L4** is not new and the characterization is in agreement with the literature report by Vance *et al.*[56] (ESI-Fig. 8 and 9†). The new **L5** was isolated as a white solid only soluble upon deprotonation using aqueous NaOH. All the expected characteristic protons of **L5** have been depicted in the proton NMR spectrum (ESI-Fig. 10†). FT-IR spectroscopy further confirmed the functional groups, with the carboxylic O–H stretching and C=O stretching vibrating at 3096 cm^{-1} ν(O–H) and the carbonyl at 1680 ν(C=O) cm^{-1}, whereas the imine stretchings vibrated at 1598 cm^{-1} ν(C=N) and 1572 cm^{-1} ν(C=N).

The corresponding palladium complexes (**C1–C5**) were also isolated. This was achieved by following the reaction conditions outlined in Fig. 3 and 4. The proton NMR spectrum of **C1** revealed all the expected characteristic peaks, which include those of the counter ion –BPh_4 signalling between 6.04 ppm and 7.28 ppm accounting for 20 protons (ESI-Fig. 11†). The phosphorus NMR spectrum depicted a singlet at 35.5 ppm which is a downfield shift from 9.9 ppm **L1**, which is an expected shift upon coordination with the palladium centre.[57] The mass spectrum of **C1** revealed $m/z = 798.1198$ $[M]^+$.

C2 has different solubility from that of **L2**, which suggests that the coordination with the Pd centre improved the solubility. However, this difference in solubility also provides evidence that we have successfully isolated **C2** with the proton NMR confirming all the characteristic signals (ESI-Fig. 12†). FT-IR spectroscopy revealed a shift from 1595 cm^{-1} (**L2**) to 1581 cm^{-1} (**C2**) for ν(C=N) and a shift from 1363 cm^{-1} (**L2**) to 1242 cm^{-1} (**C2**) for ν(P=N) as a result of π backdonation of electrons (metal-to-ligands). This is further supported by the mass spectrum which depicted the parent ion, $m/z = 888.0969$ $[M]^+$ (ESI-Fig. 13†). The purity of **C2** was also confirmed by the elemental analysis; % calculated = C 58.55 H 4.04 N 4.55, and % results = C 59.24 H 4.16 N 3.99.

Moreover, **C3** was isolated as a peach solid which is soluble in chlorinated solvents, DMSO, DMF and THF. The isolation of **C3** was further confirmed by proton NMR which depicted all the expected characteristic signal peaks (Fig. 5). The ^{13}C NMR spectrum of **C3** revealed the most deshielded carbon at 166.6 ppm which is assigned to the carbonyl quaternary carbon. The phosphorus NMR spectrum also revealed a shift from 7.80 ppm (**L3**) to 40.36 ppm (**C3**), which also confirms that the palladium centre has coordinated successfully. Furthermore, the mass spectrum depicted the parent ion $m/z = 944.1520$ $[M]^+$.

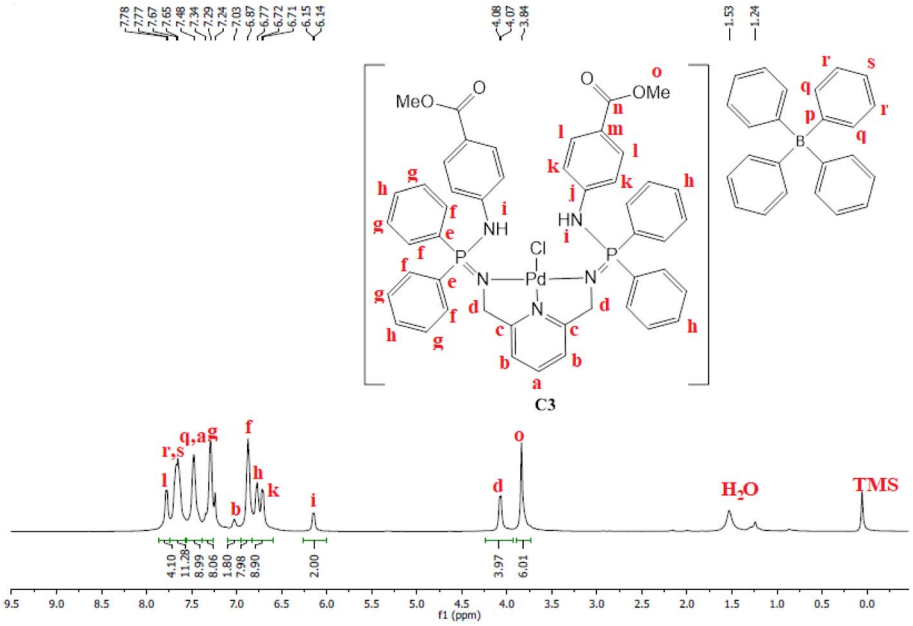

Fig. 5 The ^{1}H NMR spectra of **C3** recorded in $CDCl_3$ at 25 °C.

C4 was isolated as a green solid, confirmed using the mass spectrum which depicted the parent ion m/z = 499.0456 $[M]^+$. Upon coordination of the Pd centre to **L4** the imine stretching frequency bands shifted from 1566 cm^{-1} ν(C=N) and 1620 cm^{-1} ν(C=N) to lower wavenumbers 1550 cm^{-1} ν(C=N) and 1589 cm^{-1} ν(C=N) thus confirming isolation of **C4**. This observation agrees with similar reports in the literature for Pd centres coordinated to Schiff base imines.[58,59]

C5 revealed the most deshielded broad proton signals at 12.22 ppm integration for two protons assigned to –O*H*, a broad signal at 8.22 ppm assigned to the imine protons integrating for two protons, followed by the aromatic protons in the region 5.86 ppm to 7.84 ppm assigned to Ar–*H* integrating for 11 protons (ESI-Fig. 15†). The ^{13}C NMR spectrum of **C5** also revealed all the characteristic signals (ESI-Fig. 16†).

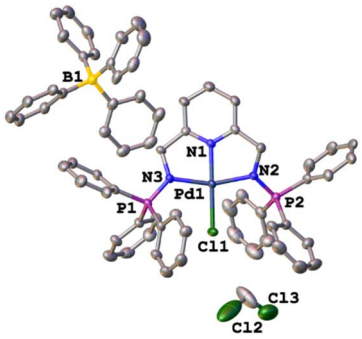

Fig. 6 The crystal structure of **C1**. The protons were removed for clarity. Selected bond distances (Å) and bond angles (°). Pd(1)–Cl(1) 2.298(12), Pd(1)–N(1) 1.940, Pd(1)–N(2) 2.042(4), Pd(1)–N(3) 2.044(4), P(2)–N(2) 1.599(4), P(1)–N(3) 1.598(4) and N(2)–Pd(1)–Cl(1) 99.4(11), N(3)–Pd(1)–Cl(1) 99.1(11), N(1)–Pd(1)–Cl(1) 177.1(11), and N(3)–Pd(1)–N(2) 161.5(15).

The single crystal X-ray molecular structure of C1

The green single crystals of the **C1** complex were grown in DCM through slow evaporation of the complex to further confirm the structure of **C1** with traces of the DCM solvent. The crystallographic data and molecular structure are given in ESI-Table 1† and Fig. 6. Complex C1 crystalized in a monoclinic system, space group $P2_1/c$. The bond distances and angles around the palladium centre show similarities to those reported in the literature for similar palladium complexes.[59–62] The observed bond distances for **C1** (Fig. 5) Pd(1)–N(1) 1.940, Pd(1)–N(2) 2.042(4), and Pd(1)–N(3) 2.044(4) are in agreement with those reported by Jerome *et. al.*[63] for the Pd(II)–NNN pincer complex reporting Pd(1)–N(1) 2.028(3), Pd(1)–N(2) 1.920(3), and Pd(1)–N(3) 2.035(3). Similarly, the selected bond angle for **C3** N(3)–Pd(1)–N(2) 161.5(15) is similar to that of N(1)–Pd(1)–N(3), 160.68(12) from the Pd(II)–NNN pincer complex.[63]

Catalytic hydrogenation of furfural to furfuryl alcohol

The hydrogenation of FFR to FFA requires the presence of a pre-catalyst, base, hydrogen source (*e.g.* formic acid (FA)), solvent or solvent-free conditions, and heat (Fig. 7). This can be achieved successfully through the evaluation of optimum conditions which also include reaction time.

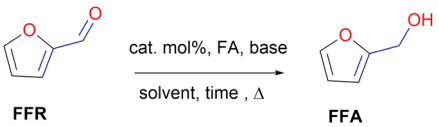

Fig. 7 The hydrogenation of FFR to FFA.

Table 1 The evaluation of optimum reaction conditions for the hydrogenation of FFR to FFA, using pre-catalysts **C1** and **C2** respectively

Entry	Cat.	H-source	Temp. (°C)	Conv. (%)	TON	TOF (h^{-1})	FFA (mmol) (yield%)	FF-formate (mmol)
1	**C1**	FA	120	68	680	136	3.391 (68)	0.0324
2	**C2**	FA	120	63	630	126	3.158 (63)	0.0454
3	**C1**	FA	130	90	900	180	4.358 (87)	0.123
4	**C2**	FA	130	85	850	170	4.144 (83)	0.441
5	**C1**	FA	140	84	840	168	3.858 (77)	0.363
6	**C2**	FA	140	88	880	176	4.335 (87)	0.272
7	**C1**	FA	150	96	960	192	4.715 (94)	0.181
8	**C2**	FA	150	96	960	192	4.759 (95)	0.104
9	**C1**	FA	160	99	990	198	4.896 (98)	0.0778
10	**C2**	FA	160	98	980	196	4.702 (94)	0.194
11	**C1**	EtOH	150	—	—	—	—	—
12	**C2**	EtOH	150	18	180	36	0.182 (4)	—
13	**C1**	iPrOH	150	—	—	—	—	—
14	**C2**	iPrOH	150	—	—	—	—	—

[a] Reaction conditions: reactions were carried out in formic acid/ethanol/isopropanol (5 mmol) with 5 mmol of FFR, 5 mmol of base Et_3N and 0.1 mol% Pd catalyst loading (**C1**/**C2**). The reaction was allowed to run for 5 hours at 120–160 °C. Thereafter, DMF was used as an internal standard, and TONs and mmol product were determined by ^1H NMR spectroscopy. Products were confirmed by GC-MS (ESI-Fig. 19 and 20).

The evaluation of optimum reaction conditions

The investigation of optimum conditions was conducted under solvent-free conditions. The effects of temperature (entry 1–8) using triethylamine as a base and FA as the hydrogen source were evaluated (Table 1). The conversions and amount of product formed increased significantly from 120–150 °C thus giving 63–98% for **C1** and **C2** respectively. While the conversions differ by ~3%, the difference in the amount (in mmol) of FFA produced is negligible (Table 1, entries 7–10) as the amounts are more or less similar for temperatures 150 °C and 160 °C. Therefore, an optimum temperature of 150 °C with potential minimal energy saving compared to 160 °C was selected. When alcohols such as ethanol and isopropanol were utilized as hydrogen sources (Table 1, entries 11–14), ethanol showed some activity when **C2** was used as a pre-catalyst, but isopropanol did not. Formic acid is the optimum hydrogen source with up to 98% conversions. It is speculated that the presence of the carboxylic acid group on **C2** has some influence on these catalytic systems as observed in the reaction where ethanol was used as the hydrogen source giving 0.182 mmol furfuryl alcohol (18% conversion).

The base evaluation includes the use of triethylamine (Et_3N), potassium hydroxide (KOH), sodium bicarbonate ($NaHCO_3$) and pyridine (Fig. 8). Et_3N was the only active base with 96% conversion in 5 hours for both **C1** and **C2** respectively. The selectivity favours the formation of FFA; however, there seem to be some traces of furfuryl formate. The effects of reaction time on FFA production using **C1** were evaluated (Fig. 9). At 1 hour only 43% of FFR followed the exponential increase to 89% after 3 hours. The conversion of FFR gradually increased from 94–100% when reaction time was increased from 4–7 hours, with no significant difference between 6 hours and 7 hours. There were no traces of furfuryl formate produced at 6 hours (ESI-Fig. 17†). Therefore, the optimum reaction time was chosen at 6

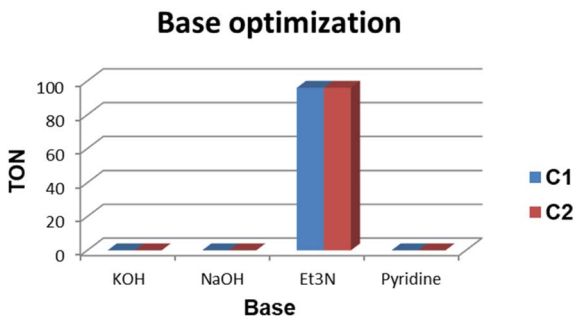

Fig. 8 Reaction conditions: reactions were carried out in FA (5 mmol) with 5 mmol of FFR and 5 mmol of base (Et_3N/KOH/pyridine/$NaHCO_3$ and 0.1 mol% Pd catalyst loading (**C1**/**C2**). The reaction was allowed to run for 5 hours at 120–160 °C. Thereafter, DMF was used as an internal standard, and TONs and mmol product were determined by ^1H NMR spectroscopy.

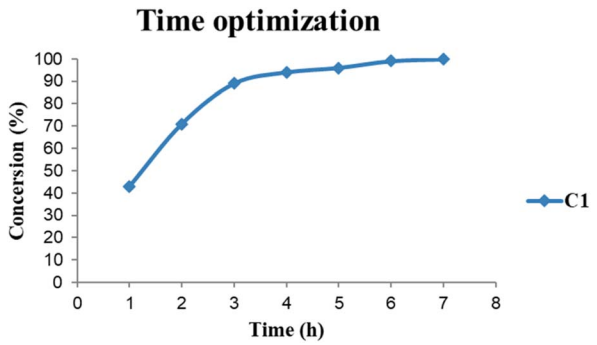

Fig. 9 Reaction conditions: Reactions were carried out in FA (5 mmol) with 5 mmol of FFR, 5 mmol of Et_3N and 0.1 mol% Pd catalyst loading **C1**. The reaction was allowed to run for 1–7 hours at 150 °C. DMF was used as an internal standard, and TONs and mmol product were determined by ^1H NMR spectroscopy.

Table 2 The effects of catalyst variation (**C1–C5**) and catalyst loading on conversion of FFR to FFA

Entry	Cat.	Cat. mol%	Conv. (%)	TON	TOF (h^{-1})	FFA (mmol) (yield%)	FF-formate (mmol)
1	**C1**	0.1	>99	1000	167	5.000 (100)	—
2	**C2**	0.1	>99	999	166	4.996 (99)	0.00227
3	**C3**	0.1	>99	1000	167	4.998 (>99)	—
4	**C4**	0.1	>99	997	166	4.996 (>99)	—
5	**C5**	0.1	>99	999	166	4.998 (>99)	—
6	**C1**	0.05	>99	1999	333	4.997 (>99)	—
7	**C1**	0.025	>99	4001	667	4.998 (>99)	—
8	**C1**	0.01	>99	9996	1666	4.998 (>99)	—
9[b]	—		>99			4.997 (>99)	—
10[b,c]	—	—	45			1.664 (33)	0.5945
11[b,d]	—	—	28			0.8490 (17)	0.5650
12[b,e]	—	—	27			1.254 (25)	0.1292
13[b,f]	—	—	0			0	0
14[b,g]	—	—	0			0	0

[a] Reaction conditions: Reactions were carried out in FA (5 mmol) with 5 mmol of FFR and 5 mmol of Et_3N using pre-catalysts **C1–C5** respectively. The reaction was allowed to run for 6 hours at 150 °C. DMF was used as an internal standard, and TONs and mmol product were determined by ^1H NMR spectroscopy. [b] No metal-catalyst was used. [c] 2.5 mmol FA and 2.5 mmol Et_3N. [d] 2.5 mmol FA and 0.007 mmol Et_3N. [e] 2.5 mmol FA. [f] No FA. [g] No Et_3N.

hours with 100% conversions. Literature reports mostly use hydrogen gas (H_2) as a hydrogen source and this often requires higher temperatures, a solvent and/or longer reaction times. Wang and colleagues used supported monometallic catalysts in the hydrogenation of FFR at temperatures ranging from 200–260 °C, at 30 bar H_2 in isopropanol over 5 hours. They obtained up to 95% conversion and the reaction was unselective, producing five different products.[25] Our research group has also explored H_2 as a hydrogen source in furfural hydrogenation using Pd(II), Pt(II), and Ni(II) homogeneous and heterogeneous catalysts. In the presence of a solvent such as ethanol, 100% conversions were recorded in 24 hours producing FFA selectively.[35,39,64] Herein, we report the use of moderate temperatures and shorter reaction times.

The effects of catalyst variation

The pre-catalyst variation revealed no significant difference in conversion with all the catalysts **C1–C5** giving conversion of greater than 99% (TON ≈ 167) (Table 2, entry 1–5). No traces of furfuryl formate (FF-formate) were produced when **C1** and **C3–C5** were used respectively. The homogeneity of catalysts **C1–C5** was evaluated using the mercury poisoning test. This was achieved by introducing 5 mg of mercury (Hg) into the catalytic systems. All catalysts revealed no change in conversions of FFR to FFA, maintaining >99% (ESI-Fig. 18†), thus confirming no leaching of the catalysts and suggesting that **C1–C5** are homogeneous catalysts.

We then went on to evaluate the catalyst loading using **C1**. Decreasing the catalyst loading from 0.1 mol% to 0.01 mol% did not affect the conversions as they remained greater than 99% (TON ≈ 9996); however the traces of furfuryl formate were no longer observed (Table 2, entry 6–8). Surprisingly, upon omitting the metal-catalyst the efficiency of the optimum conditions maintained a conversion of >99% with an FFA production of 4.997 mmol (Table 2, entry 9).

Upon using half the amount of FA and Et_3N to 2.5 mmol respectively, the conversion decreased to 45% (Table 2, entry 10). Furthermore, lowering the amount of FA by half (2.5 mmol) and Et_3N to 0.007 mmol the conversion significantly dropped to 28% (Table 2, entry 11). Lowering just the amount of FA by half (2.5 mmol) and maintaining Et_3N at 5.0 mmol resulted in a conversion of 27% (Table 2, entry 12). Moreover, performing the reaction without FA resulted in no conversion (Table 2, entry 13). Subsequently, perfomung the reaction in the absence of Et_3N resulted in no conversion (Table 2, entry 14). These observations suggest that formate mediated FFR hydrogenation to FFA is a stoichiometric reaction. Thus, the optimum conditions to convert FFR to FFA were 5.00 mmol each of FFR, FA and Et_3N at 150 °C over 6 hours. This prompted us to use formate-facilitated conversion of FFR to FFA using different amines to generate formate from formic acid *in situ*. This was performed using a new birch reactor and a new stirrer bar.

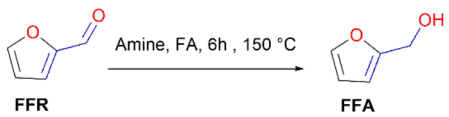

Fig. 10 The organocatalyzed hydrogenation of FFR to FFA.

Table 3 Effects of various amines on the conversion of FFR to FFA

Entry	Amine	Conv.%	mmol FFA
1	Et_3N	>99	4.997
2	Et_2NH	>99	4.999
3	Pyrrolidine	>99	4.999
4	*N-N*-Dimethylethylamine	>99	4.994

[a] Reaction conditions: reactions were carried out in formic acid (5 mmol) with 5 mmol of FFR and 5 mmol of amine. The reaction was allowed to run for 6 hours at 150 °C. DMF was used as an internal standard, and the mmol product was determined by ^1H NMR spectroscopy.

Prior to this work, our research group studied several metal catalysts which include palladium, platinum, nickel, ruthenium and iridium (homogeneous and heterogenized homogeneous catalysts) which were found to be necessary for the hydrogenation of FFR. This includes the study by Oklu *et al.*[34] where they used homogeneous iridium and ruthenium half–sandwich complexes as catalyst precursors under solvent-free conditions in the presence of Et_3N and formic acid. The authors reported TONs of up to 2961. Recently, Anyomih *et al.*[36] used a homogeneous palladium(II) pyrazolyl catalyst also under solvent-free conditions in the presence of Et_3N and formic acid, to achieve up to 95% FFR conversions to FFA in 6 hours at 160 °C. In this study, we initially evaluated palladium catalysts in FFR hydrogenation, in efforts to improve efficiency. During this study we discovered that the control blank catalytic run (without the palladium catalysts) proceeded to give FFA under solvent-free conditions. As such, this article reports this new methodology – metal catalyst free FFR hydrogenation, with an expansion to other aldehydes.

The hydrogenation of furfural using various amines and formic acid

FFR can be converted to FFA in the presence of triethylamine (Et_3N) and formic acid at 150 °C in 6 hours (Fig. 10). Various

Table 4 The hydrogenation of various aldehydes to their corresponding alcohols and formates

Entry	Aldehyde	Conv. (%)	mmol product (yield%)	mmol formate (yield%)
1	 Benzaldehyde	86.9	3.994 (79.7) 	0.359 (7.19) 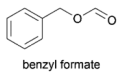 benzyl formate
2	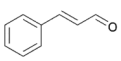 cinnamaldehyde	69.4	3.472 (69.4) 	—
3	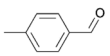 4-Methylbenzaldehyde	59.5	1.265 (25.3) 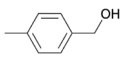	2.252 (45.0) 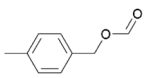 4-methylbenzyl formate
4	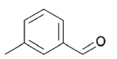 3-Methylbenzaldehyde	71.1	1.302 (26.0) 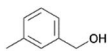	2.252(45.1) 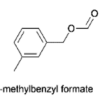 3-methylbenzyl formate
5	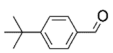 4-Tertbutylbenzaldehyde	72.2	2.234 (44.7) 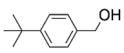	1.373 (27.5) 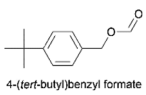 4-(*tert*-butyl)benzyl formate
6	 Thiophene-2-carboxaldehyde	85.4	4.269 (85.4) 	—
7	 Pyridine-2-carboxaldehyde	100	5.000 (100) 	—
8	 4-Formylbenzoic acid	0	—	—
9	 Propionaldehyde	79.8	3.99 (79.8) 	—
10	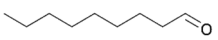 Nonanal	89.0	3.49 (69.9) 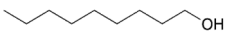	0.9589 (19.2)
11	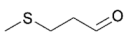 3-(methylthio) propionaldehyde	100	5.00 (100) 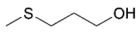	—

[a] Reaction conditions: reactions were carried out in formic acid (5 mmol) with 5 mmol aldehyde and 5 mmol of Et_3N. The reaction was allowed to run for 6 hours at 150 °C. DMF was used as an internal standard, and the mmol product was determined by ^1H NMR spectroscopy. GC-MS was also used to further confirm the products (ESI-Fig. 21–29).

amines were also evaluated such as diethylamine, pyrrolidine, and *N*-*N*-dimethylethylamine (Table 3). This system responds optimally when these secondary and tertiary amines are used giving up to >99% conversions and a percentage yield of FFA. In this study, triethylamine has been chosen because it is most used in our laboratories and therefore always available for use.

The organocatalyzed stoichiometric hydrogenation of various aldehydes

Using the optimum conditions, various aldehydes were screened for their ability to convert to their respective alcohols and formates (Table 4, entry 1–11). The conversion of benzaldehyde was achieved at 87% selectivity to benzyl alcohol and benzyl formate with yields of 80% and 7% respectively (Table 4, entry 1). Cinnamaldehyde as a substrate was only selective to cinnamyl alcohol with 69% conversion achieved (Table 4, entry 2). 4-Methylbenzaldehyde and 3-methylbenzaldehyde have methyl groups on the *para* and *meta* positions respectively affording conversions of 59% and 71% encouraged by the deactivating group's (CHO) preference for meta directors (Table 4, entries 3 and 4). When the bulkier *para*-substituted 4-tert-butylbenzaldehyde was utilized as a substrate, it exhibited a higher conversion of 72% specifically to 4-*tert*butylbenzyl alcohol and 4-*ter*tbutylbenzyl formate (Table 4, entry 5). The respective conversions of thiophene-2-carboxaldehyde and pyridine-2-carboxaldehyde obtained were 85% and 100% selective to only the corresponding alcohols (Table 4, entry 6 and 7). 4-Formylbenzoic acid as a substrate showed no activity, which may be due to the electron withdrawing group (carboxylic group) competing with the aldehyde (Table 4, entry 8).

Linear substrates such as propionaldehyde, nonanal and 3-(methylthio)propionaldehyde were also evaluated and achieved good conversions of 80% (propanol), 89% (nonanol) and 100% (3-(methylthio)propanol) (Table 4, entry 9–11). The evaluation of various aldehydes was successful, affording the corresponding alcohols. However, upon attempts to use the optimum conditions on other carbonyl compounds such as ketones and carboxylic acids, no activity was observed.

Conclusions

The catalytic hydrogenation of furfural to furfuryl alcohol was investigated using iminophosphorane and pyridyl imine palladium pincer complexes (**C1–C5**). Furfural was converted to furfuryl alcohol in the presence of triethylamine (Et_3N) and formic acid (FA) at 150 °C in 6 hours with a catalyst loading of 0.1 mol% obtaining conversions of >99%. However, by lowering the catalyst loading to 0.01 mol% all the pre-catalysts maintained the same conversions of >99%. Without the metal-catalyst, the optimum conditions retained the conversions of >99% with furfuryl alcohol. This observation led to a new procedure which encouraged the evaluation of an organocatalyzed variety of aldehydes to their respective alcohols which was successfully achieved under the stoichiometric solvent-free conditions.

Author contributions

Asanda C. Matsheku: conceptualization, methodology, investigation, writing of the original draft and visualization. Munaka Christopher Maumela: co-supervision, conceptualization, validation, and writing-review and editing. Banothile C. E. Makhubela: supervision, conceptualization, methodology, writing—review and editing, project administration and validation. All authors have read and agreed to the published version of the manuscript.

Conflicts of interest

The authors declare no conflict of interest.

Acknowledgements

This research was funded by the National Research Foundation of South Africa (NRF) (Grant Numbers: 117989 and 131253). We also give our appreciation to the University of Johannesburg (UJ) Centre for Synthesis and Catalysis, UJ Faculty of Science Spectrum for the use of facilities.

References

1 J. J. Bozell and G. R. Petersen, *Green Chem.*, 2010, **12**, 539–554.
2 A. Corma, S. Iborra and A. Velty, *Chem. Rev.*, 2007, **107**, 2411–2502.
3 F. W. Lichtenthaler, *Carbohydr. Res.*, 1998, **313**, 69–89.
4 W. L. Kubic, X. Yang, C. M. Moore and A. Sutton, *Chemicals from Biomass: a Market Assessment of Bioproducts with Near-Term Potential*, 2020.
5 M. J. Biddy, C. J. Scarlata and C. M. Kinchin, *Chemicals from Biomass: A Market Assessment of Bioproducts with Near-Term Potential*, 2016.
6 *Large Scale Furfural Production (from Bagasse)*, **https://dalinyebo.com/project/large-scale-furfural-production-from-bagasse/**, accessed 31 August 2022.
7 X. Li, P. Jia and T. Wang, *ACS Catal.*, 2016, **6**, 7621–7640.
8 J. N. Chheda, G. W. Huber and J. A. Dumesic, *Angew. Chem., Int. Ed.*, 2007, **46**, 7164–7183.
9 K. Yan, G. Wu, T. La and C. Jarvis, *Renew. Sustain. Energy Rev.*, 2014, **38**, 663–676.
10 J. C. Serrano-Ruiz, R. Luque and A. Sepulveda-Escribano, *Chem. Soc. Rev.*, 2011, **40**, 5266–5281.
11 J. Lee, Y. T. Kim and G. W. Huber, *Green Chem.*, 2014, **16**, 708–718.
12 G. J. S. Dawes, E. L. Scott, J. Le Nôtre, J. P. M. Sanders and J. H. Bitter, *Green Chem.*, 2015, **17**, 3231–3250.
13 M. J. Climent, A. Corma and S. Iborra, *Green Chem.*, 2014, **16**, 516–547.
14 R. Rao, A. Dandekar, R. T. K. Baker and M. A. Vannice, *J. Catal.*, 1997, **171**, 406–419.
15 H. E. Hoydonckx, W. M. Van Rhijn, W. Van Rhijn, D. E. De Vos and P. A. Jacobs, in *Ullmann's Encyclopedia of Industrial Chemistry*, Wiley-VCH, Weinheim, 2007, p. 14356007.

16 Á. O. Driscoll, J. J. Leahy and T. Curtin, *Catal. Today*, 2017, **279**, 194–201.
17 C. M. Peeters and R. Deliever, *J. Chem. Ed.*, 2009, **86**, 87–90.
18 J. Magano and J. R. Dunetz, *Org. Process Res. Dev.*, 2012, **16**, 1156–1184.
19 A. Berkessel, T. J. S. Schubert and T. N. Müller, *J. Am. Chem. Soc.*, 2002, **124**, 8693–8698.
20 C. Walling and L. Bollyky, *J. Am. Chem. Soc.*, 1964, **86**, 3750–3752.
21 C. Walling and L. Bollyky, *J. Am. Chem. Soc.*, 1961, **83**, 2968–2969.
22 W. Gong, C. Chen, R. Fan, H. Zhang, G. Wang and H. Zhao, *Fuel*, 2018, **231**, 165–171.
23 W. Ouyang, A. Yepez, A. A. Romero and R. Luque, *Catal. Today*, 2018, **308**, 32–37.
24 B. Wang, C. Li, B. He, J. Qi and C. Liang, *J. Energy Chem.*, 2017, **26**, 799–807.
25 Y. Wang, P. Prinsen, K. S. Triantafyllidis, S. A. Karakoulia, P. N. Trikalitis, A. Yepez, C. Len and R. Luque, *ACS Sustain. Chem. Eng.*, 2018, **6**, 9831–9844.
26 L. Grazia, A. Lolli, F. Folco, Y. Zhang, S. Albonetti and F. Cavani, *Catal. Sci. Technol.*, 2016, **6**, 4418–4427.
27 S. Wang, V. Vorotnikov and D. G. Vlachos, *Green Chem.*, 2014, **16**, 736–747.
28 S. Sitthisa, W. An and D. E. Resasco, *J. Catal.*, 2011, **284**, 90–101.
29 S. Sitthisa, T. Sooknoi, Y. Ma, P. B. Balbuena and D. E. Resasco, *J. Catal.*, 2011, **277**, 1–13.
30 R. Mariscal, P. Maireles-Torres, M. Ojeda, I. Sadaba and M. Lopez Granados, *Energy Environ. Sci.*, 2016, **9**, 1144–1189.
31 G. Singh, L. Singh, J. Gahtori, R. Kumar, C. Samanta, R. Bal and A. Bordoloi, *Mol. Catal.*, 2021, **500**, 111339.
32 D. Liu, D. Zemlyanov, T. Wu, R. J. Lobo-Lapidus, J. A. Dumesic, J. T. Miller and C. L. Marshall, *J. Catal.*, 2013, **299**, 336–345.
33 J. M. Tukacs, M. Bohus, G. Dibó and L. T. Mika, *RSC Adv.*, 2017, **7**, 3331–3335.
34 N. K. Oklu and B. C. E. Makhubela, *New J. Chem.*, 2020, **44**, 9382–9390.
35 P. S. Moyo, L. C. Matsinha and B. C. E. Makhubela, *J. Organomet. Chem.*, 2020, **922**, 121362.
36 W. D. Anyomih, N. K. Oklu, E. Ocansey, K. K. Singh, J. Darkwa and B. C. E. Makhubela, *Biomass Convers. Biorefin.*, 2022, DOI: 10.1007/s13399-022-03449-2.
37 N. Gorgas, B. Stöger, L. F. Veiros and K. Kirchner, *ACS Catal.*, 2016, **6**, 2664–2672.
38 A. Mukherjee and D. Milstein, *ACS Catal.*, 2018, **8**, 11435–11469.
39 M. Kalumpha, L. C. Matsinha and B. C. E. Makhubela, *Catalysts*, 2021, **11**, 1–22.
40 S. Murugesan and K. Kirchner, *Dalton Trans.*, 2016, **45**, 416–439.
41 M. Albrecht and G. Van Koten, *Angew. Chem, Int. Ed.*, 2001, **40**, 3750–3781.
42 R. A. Gossage, L. A. Van De Kuil and G. Van Koten, *Acc. Chem. Res.*, 1998, **31**, 423–431.
43 M. E. van der Boom and D. Milstein, *Chem. Rev.*, 2003, **103**, 1759–1792.
44 J. T. Singleton, *Tetrahedron*, 2003, **59**, 1837–1857.
45 L. C. Liang, *Coord. Chem. Rev.*, 2006, **250**, 1152–1177.
46 S. Ramírez-rave, D. Morales-morales and J. Grévy, *Inorg. Chim. Acta.*, 2017, **462**, 249–255.
47 G. K. Anderson, M. Lin, A. Sen and E. Gretz, in *Inorganic Syntheses*, John Wiley & Sons, Inc., Hoboken, NJ, USA, 2007, pp. 60–63.
48 Bruker-AXS, SADABS, *S. S. R. Manuals and M. U. Wisconsin*, 2009.
49 G. Sheldrick and A. Shelxl, *Sect. A Fundam. Crystallogr.*, 2008, **64**, 112–122.
50 H. Su, C. Wu, J. Zhu, T. Miao, D. Wang, C. Xia, X. Zhao, Q. Gong, B. Song and H. Ai, *Dalton Trans.*, 2012, **41**, 14480–14483.
51 T. Cheisson and A. Auffrant, *Dalton Trans.*, 2014, **43**, 13399–13409.
52 K. C. Nicolaou, C. N. C. Boddy, H. Li, A. E. Koumbis, R. Hughes, S. Natarajan, N. F. Jain, J. M. Ramanjulu, S. Bräse and M. E. Solomon, *Chem.–Eur. J.*, 1999, **5**, 2602–2621.
53 K. C. Nicolaou, N. F. Jain, S. Natarajan, R. Hughes, M. E. Solomon, H. Li, J. M. Ramanjulu, M. Takayanagi, A. E. Koumbis and T. Bando, *Angew. Chem., Int. Ed.*, 1998, **37**, 2714–2716.
54 N. A. Bailey, D. E. Fenton, S. J. Kitchen, T. H. Lilley, M. G. Williams, P. A. Tasker, A. J. Leong and L. F. Lindoy, *J. Chem. Soc., Dalt. Trans.*, 1991, 627–637.
55 M. D. Milošević, A. D. Marinković, P. Petrović, A. Klaus, M. G. Nikolić, N. Prlainović and I. N. Cvijetić, *Bioorg. Chem.*, 2020, **102**, 104073.
56 A. L. Vance, N. W. Alcock, J. A. Heppert and D. H. Busch, *Inorg. Chem.*, 1998, **37**, 6912–6920.
57 M. Abubekerov, S. I. Khan and P. L. Diaconescu, *Organometallics*, 2017, **36**, 4394–4402.
58 A. C. Matsheku, R. Tia, M. C. Maumela and B. C. E. Makhubela, *Catalysts*, 2021, **11**, 755.
59 A. C. Matsheku, M. C. Maumela and B. C. E. Makhubela, *Polyhedron*, 2021, **205**, 115280.
60 V. Diez, V. Cuevas, G. Garcı, G. Aullo, J. P. H. Charmant, U. De Burgos and P. M. Ban, *Inorg. Chem.*, 2007, **46**, 2220–2222.
61 R. Wang, J.-C. Xiao, B. Twamley and J. M. Shreeve, *Org. Biomol. Chem.*, 2007, **5**, 671.
62 J. G. P. Delis, M. Rep, R. E. Rülke, P. W. N. M. van Leeuwen, K. Vrieze, J. Fraanje and K. Goubitz, *Inorg. Chim. Acta.*, 1996, **250**, 87–103.
63 P. Jerome, J. Haribabu, N. S. P. Bhuvanesh and R. Karvembu, *ChemistrySelect*, 2020, **5**, 13591–13597.
64 P. S. Moyo, B. Vatsha, G. Mehlana, L. C. Matsinha and B. C. E. Makhubela, *Dalton Trans.*, 2023, **52**, 6300–6316.